Faraday Discussions

Cite this: *Faraday Discuss.*, 2017, **196**, 43

PAPER

View Article Online
View Journal | View Issue

Polyurethanes with aggregation-enhanced emission characteristics: preparation and properties†

Kun Wang, Jiping Yang,* Chen Gong and Hao Lu

Received 2nd August 2016, Accepted 25th August 2016
DOI: 10.1039/c6fd00175k

An amino-terminated poly(propylene glycol)-modified tetraaryl-buta-1,3-diene derivative (TABDAA) was introduced to synthesize polyurethanes with different ratios of soft/hard segments. A mixture of TABDAA and poly(tetrahydrofuran) 1000 as the soft segments was reacted with 4,4-diphenylmethane diisocyanate and 1,4-butanediol as the hard segments in molar ratios of 1 : 2 : 1, 2 : 3 : 1, and 3 : 4 : 1 to give the desired polyurethanes named TMPU-211, TMPU-321 and TMPU-431, respectively. The three polyurethanes exhibited different aggregation-enhanced emission (AEE) behaviors because of their different soft/hard segment ratios. The polyurethanes with a higher soft segment content tended to form bigger particles in a DMF/water mixture solution, thus causing a sharper increase in their fluorescence intensity. In addition, the polyurethane films exhibited different fluorescence intensities after different heat treatments. After a quenching treatment of the soft segments in the polyurethane films, the fluorescence intensity dropped greatly. When these quenched polyurethane films were thermally annealed at 60 °C for 24 hours, their fluorescence intensity exceeded the initial intensity of the as-prepared films. Differential scanning calorimetry results showed that the polyurethane films in the quenched condition did not present the endothermal melting peak of the soft segments, and the melting peaks appeared again after thermal annealing. AFM experiments showed that an ordered arrangement was achieved after the heat treatment of these AEE polyurethane films. These results demonstrated that the polymer structure had a significant effect on the AEE properties of the polyurethane films, and more importantly, it is of great significance in improving the fluorescence emission of the AEE polymers and also for their potential application in fluorescent probes, stimuli-responsive materials, PLED devices and so on.

Key Laboratory of Aerospace Advanced Materials and Performance, Ministry of Education, School of Materials Science and Engineering, Beihang University, Beijing 100083, China. E-mail: jyang@buaa.edu.cn; Tel: +86-010-82338955

† Electronic supplementary information (ESI) available. See DOI: 10.1039/c6fd00175k

1. Introduction

As an excellent solution to fluorescence-quenching problems encountered in the aggregation state, aggregation-induced emission (AIE) has attracted much attention since it was first reported in 2001.[1] Such AIE molecules are marked with a characteristic property, that is, they are non-luminescent or faintly luminescent when dissolved in solution but are able to emit fluorescence when aggregated in poor solvents or the solid state. This phenomenon directly contrasts with the well-known aggregation-caused quenching behavior encountered in the condensed states, providing an ideal solution to this fluorescence-quenching problem under aggregate conditions.

When it comes to practical applications, AIE molecules are often integrated into a polymer matrix, which leads to better stretchability, better mechanical strength and more possibility for chemical modulation. Thus this field is growing magnificently, and much progress has been achieved so far. Specifically, most of the AIE polymers are based on AIE small molecules, such as tetraphenylene,[2] tetraphenylthiophene,[3] 9,10-dis-tyrylanthracene[4] *etc*, in which linear AIE polymers are prepared with AIE fluorophores in their side chains[5–10] or main chains.[11–17] It should be noted that most linear polymers integrated with AIE molecules are observed to have aggregation-enhanced emission (AEE) characteristics, that is, the polymers are slightly emissive in solution, which is different from the absolute fluorescence extinction found in AIE molecules.[18,19] The obvious reason for this interesting phenomenon is the restriction of the AIE fluorophore by the polymer matrix. Restricted intramolecular rotation (RIR) has been suggested as the possible origin of the AIE phenomenon, that is, in an aggregated state, such as nanoparticles and solid thin films/powders, the molecules are in crowded surroundings and thus intramolecular motions are restricted, which diminishes the non-radiative decay of the excited state energy and consequently induces strong emission. As for AIE/AEE polymer solutions, the polymer chain can effectively hinder the intramolecular rotation of the fluorophores, leading to a higher emission yield in both the aggregates and the solution compared to the organic molecules. To the best of our knowledge, it is the polymer matrix that influences the fluorescence emission state of the AIE fluorophore in the AEE polymer. However, there has been little research on the mechanism of how the structure of the polymer matrix affects the fluorescence emission of the AIE molecules.

In addition, a new kind of AIE molecule, 4,4′-((Z,Z)-1,4-diphenylbuta-1,3-diene-1,4-diyl)dibenzoic acid (TABD–COOH), was first synthesized by Dong *et al.* and exhibited nice AIE properties in 2013.[20] It was then used to prepare metal–organic frameworks which were highly sensitive and selective for the detection of explosives.[10] Other compounds derived from the TABD molecule proved to be mechanochromic AEE materials.[21] However, all of the research on TABD derivatives is based on small molecules, and AIE/AEE polymers based on a TABD core have barely been reported until now.

In this contribution, three AEE polyurethanes were synthesized based on the 4,4′-((1Z,3Z)-1,4-diphenylbuta-1,3-diene-1,4-diyl)dibenzaldehyde (TABDAA) moiety with different soft/hard segment ratios. These three polyurethanes exhibited various AEE behaviors according to the soft/hard segment ratio. The soft segments including TABDAA in the polyurethane films were then processed successively with a quenching treatment and thermal annealing. As a result, the fluorescence intensity of the films declined sharply and then finally ascended. Through systematic atomic force microscopy (AFM) and differential scanning calorimetry (DSC) characterization, it could be observed that the structure of the polymer matrix, such as the soft/hard segment ratio and condensed structure, had a great influence on the emission intensity of the AIE/AEE polyurethanes.

2. Experimental section

2.1 Materials

4-Ethynylbenzaldehyde was purchased from Sukailu Chemical Company. Palladium chloride ($PdCl_2$) and tetrakis(triphenylphosphine)palladium(0) ($Pd(PPh_3)_4$) were purchased from J&K Chemical Company. Poly(propylene glycol)bis(2-aminopropyl ether) ($M_n = 230$, D230), poly(tetrahydrofuran) ($M_n = 1000$, PTMG1000), cupric bromide ($CuBr_2$) and 4,4-diphenylmethane diisocyanate (MDI) were obtained from Aladdin Chemical Company. The PTMG1000 was dried at 105 °C under vacuum for 2 h before use. 1,4-Butanediol (BDO), tetrahydrofuran (THF), *N*,*N*′-dimethyl formamide (DMF), methylene dichloride, petroleum ether and acetonitrile were purchased from Beijing Chemical Factory. THF was dried using anhydrous magnesium sulfate for two days, then refluxed with sodium in the presence of benzophenone and distilled for use after the solvent turned blue. DMF was distilled after drying fully over calcium hydride (CaH_2). Toluene, methanol and potassium carbonate aqueous solution were degassed prior to use. All other reagents and solvents were used as commercially purchased without further purification.

2.2 Instrumentation

^{1}H-NMR spectra were obtained using a Bruker AV400 spectrometer using deuterated dimethyl sulfoxide (DMSO-d_6) as the solvent at 25 °C. Fourier transform infrared (FT-IR) spectra were recorded using a NEXUS-470 spectrometer (Nicolet) using the KBr pellet technique. UV-vis adsorption spectra were measured using a TU1901 UV-vis spectrometer at room temperature. MALDI MS spectra were obtained using Autoflex III mass spectrometers. Fluorescence spectra were obtained using a F-7000 fluorescence spectrophotometer. The molecular weight and molecular weight distribution of the polymers were determined using a Waters 150C GPC system, using THF as the eluent at a flow rate of 1.0 mL min^{-1} and a set of monodisperse polystyrenes as calibration standards. The thermal transitions of the polyurethanes were investigated using a DSC-60 Plus system at a heating rate of 10 °C min^{-1}.

2.3 Synthesis

2.3.1 (1Z,3Z)-1,4-dibromo-1,4-dibenzaldehydebuta-1,3-diene (DBDABD-CHO). 4-Ethynylbenzaldehyde was used as the raw material instead of phenylacetylene to simplify the process as illustrated in Scheme 1. 4-Ethynylbenzaldehyde (5.0 g, 0.38 mmol), $PdCl_2$ (0.34 g, 0.002 mmol), and $CuBr_2$ (25.74 g, 0.16 mmol) were added to a three-necked flask. A mixed solvent of acetonitrile (3.84 mL) and methylbenzene (192 mL) was added and the mixture was stirred at room temperature until

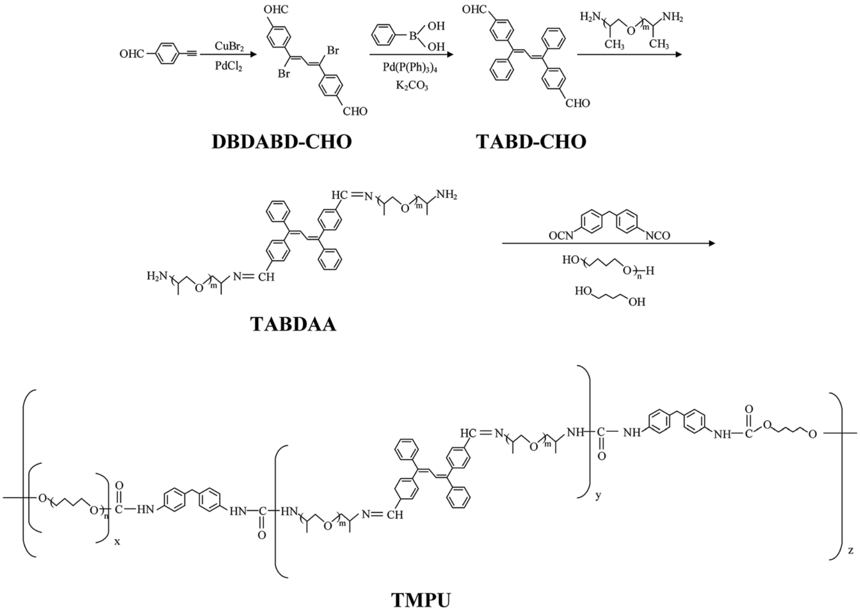

Scheme 1 Synthesis pathway of modified polyurethanes TMPU-211, TMPU-321 and TMPU-431.

complete consumption of the starting material as judged by thin layer chromatography. After the mixture was filtered and evaporated, the residue was purified by flash column chromatography using dichloromethane/petroleum ether (1 : 2) as the eluent. DBDABD-CHO was obtained as a yellow solid, with a yield of 15%. ^{1}H NMR (400 MHz, DMSO-d_6, ppm): $\delta = 10.07$ (s, 1H, CHO), 8.00 (d, 4H, Ar–H), 7.56 (s, 1H, C=C–H).

2.3.2 4,4′-((1Z,3Z)-1,4-diphenylbuta-1,3-diene-1,4-diyl)dibenzaldehyde (TABD-CHO). DBDABD-CHO (0.4 g, 0.10 mmol), phenylboronic acid (0.27 g, 2.16 mmol), Pd(PPh$_3$)$_4$ (0.06 g, 0.04 mmol) and potassium carbonate (0.79 g, 5.72 mmol) were added to a three-necked flask. Under an argon atmosphere, a mixed solvent of toluene (60 mL) and methanol (20 mL) was added and the mixture was stirred and refluxed for 24 h. After the reaction was finished, the product was extracted with CHCl$_3$ and washed with brine. The organic layers were combined and dried with MgSO$_4$. The crude product was purified by flash column chromatography using dichloromethane/petroleum ether (1 : 1) as the eluent. TABD-CHO was obtained as a yellow solid, in a yield of 85%. ^{1}H NMR (400 MHz, DMSO-d_6, ppm): 9.95 (s, 1H, CHO), 7.83 (d, 2H, Ar–H), 7.54 (m, 3H, Ar–H), 7.33 (m, 4H, Ar–H), 6.80 (s, 1H, C=C–H).

2.3.3 4,4′-((1Z,3Z)-1,4-diphenylbuta-1,3-diene-1,4-diyl)dibenzaldehyde (TABDAA). D230 (0.117 g, 0.51 mmol) was dissolved in 5 mL of chloroform in a 50 mL round bottom flask. TABD-CHO (0.1 g, 0.23 mmol) and a few drops of glacial acetic acid were dissolved in 30 mL of chloroform and added dropwise into the flask. The reaction mixture was stirred and refluxed for 24 h. After the reaction was finished, the resulting product was extracted with CHCl$_3$ and washed with brine several times. After removing the solvent by reduced pressure distillation

Table 1 Reactant molar ratios for TMPU-211, TMPU-321 and TMPU-431

Polyurethane	MDI (mmol)	PTMG1000 (mmol)	TABDAA (mmol)	BDO (mmol)
TMPU-211	15.2	7.44	0.06	7.50
TMPU-321	15.2	9.93	0.07	5.00
TMPU-431	15.2	11.17	0.08	3.75

and drying at 50 °C for 48 h under vacuum, the product was obtained as a brown yellow viscous liquid, in a yield of 63%. ^{1}H NMR (400 MHz, DMSO-d_6, ppm): 8.10–7.63 (m, 8H, Ar–H), 7.55–7.11 (m, 21H, Ar–H), 6.66 (ddd, 2H, Ar–H), 4.62–4.29 (m, 2H, –CH), 3.63–3.10 (m, 15H, $-CH_2$), 1.36–1.00 (m, 15H, $-CH_3$).

2.3.4 TMPU-211, TMPU-321 and TMPU-431. MDI and anhydrous DMF were added to the flask with magnetic stirring under a N_2 atmosphere. TABDAA was dissolved in anhydrous DMF, added to the flask and reacted at room temperature for 0.5 h. Then PTMG1000 was dissolved in anhydrous DMF and added to the mixture solution. After heating and stirring for 2 h, BDO was added dropwise and reacted for another 2 h. Finally the mixture was poured into water, and the resulting precipitates were isolated by filtration after being washed with water and ethyl alcohol several times, then put into a vacuum oven until they reached a stable weight, with a yield of ~95%. The reactant ratios for TMPU-211, TMPU-321 and TMPU-431 are listed in Table 1.

3. Results and discussion

3.1 Synthesis and characterization

We used modified procedures to prepare the TABD-CHO (as shown in Scheme 1) based on the previous literature.[22] TABD-CHO was synthesized through a typical Suzuki coupling reaction between phenylboronic acid and the bromine of DBDABD-CHO.[23] The TABDAA was prepared by the Schiff base reaction of amidocyanogen and the aldehyde groups. The detailed ^{1}H-NMR, MALDI MS and FT-IR spectra of DBDABD-CHO, TABD-CHO and TABDAA are presented in Fig. S1–S3.† Then a mixture of TABDAA and PTMG1000 was used as the soft segments, and reacted with MDI and BDO in molar ratios of 1 : 2 : 1, 2 : 3 : 1, 3 : 4 : 1 to give modified TMPU-211, TMPU-321, TMPU-431, respectively. Table 2 depicts the GPC characterization of the three modified polyurethanes, in which the three polyurethanes all have high molecular weight and low polydispersity. Moreover, the mass concentrations of TABDAA in the AEE polyurethanes were measured by a UV spectrometric method (as seen in Table 3, Fig. S4 and eqn (S1)†) and the results were in accordance with the theoretical results (0.5 wt%), proving that

Table 2 GPC characterization of the three modified polyurethanes

Polyurethane	Mn	Mw	Polydispersity
TMPU-211	51 200	95 100	1.85
TMPU-321	52 900	86 600	1.63
TMPU-431	42 600	77 400	1.81

Table 3 Mass fraction of TABDAA in the three modified polyurethanes

Polyurethane	UV absorbance	Experimental mass fraction (wt%)	Theoretical mass fraction (wt%)
TMPU-211	0.606	0.54	0.51
TMPU-321	0.490	0.44	0.51
TMPU-431	0.561	0.50	0.51

polyurethanes with the TABDAA moiety in precise proportions were synthesized successfully.

3.2 AEE feature of the modified polyurethane solutions

TMPU-211, TMPU-321 and TMPU-431 solutions with a concentration of 10.0 mg mL^{-1} were prepared. Aliquots of these polyurethane solutions were transferred to 10 mL volumetric flasks, into which appropriate volumes of DMF and water were added dropwise under vigorous stirring to furnish 1.0 mg mL^{-1} solutions with different water fractions (0–90 vol%). Then the fluorescence intensities of the modified polyurethanes in the solution mixtures were measured, and these are shown in Fig. 1a–c.

Fig. 1a shows the FL spectra of TMPU-211 solutions with different water fractions, and it can be observed that the fluorescence intensity of TMPU-211

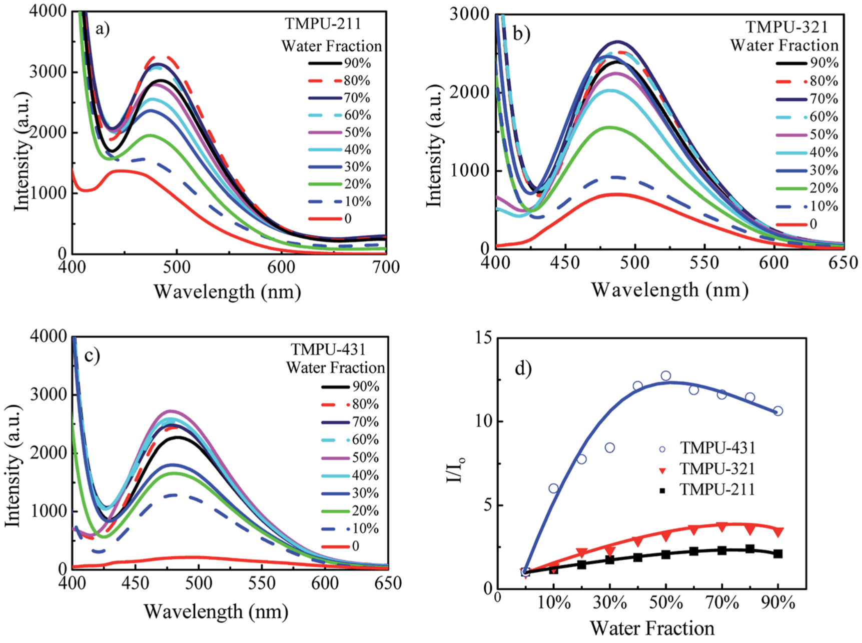

Fig. 1 Fluorescence emission spectra of: (a) TMPU-211, (b) TMPU-321, and (c) TMPU-431 in DMF/water mixtures with different water fractions; (d) relative fluorescence intensity changes recorded for the different water fractions of the three polyurethanes.

increases continuously until the water fraction is increased up to 80%. When the water fraction reached beyond 80%, the fluorescence emission started to decrease. Fig. 1b corresponds to the FL spectra of TMPU-321, in which the intensity increases gradually with the addition of water to the DMF solution. The fluorescence intensity of TMPU-321 tends to drop when the water fraction reaches more than 70%. In Fig. 1c, the highest intensity is obtained at a 50% water fraction in the TMPU-431 solution. Fig. 1d summarizes the fluorescence intensity information of the three AEE polyurethanes in a DMF/water mixture solution; obviously, there exists a common rise-first-then-fall phenomenon. Since the mass concentrations of the fluorogen in the three polyurethanes are kept the same as shown in Table 3; this indicates that the soft segment ratio plays an important role in the AEE fluorescence process. It can be found that TMPU-431 has the highest relative fluorescence intensity change, approximately 13-fold higher than that in pure DMF. The maximum fluorescence intensities of TMPU-321 and TMPU-211 are about 4-fold and 2-fold higher than the original fluorescence intensities, respectively.

To probe the changes in the aggregation state under the influence of water, polyurethane solutions with different water fractions were coated on a glass surface to give thin films after solvent evaporation. Atomic force microscopy (AFM) was used to investigate the microstructure of the polyurethane films. Fig. 2 indicates that the surface of the TMPU-321 film is rough with small nanoparticles, and these small nanoparticles are enlarged with the addition of water. According to Fig. 2a–j, the diameters of the polyurethane nanoparticles

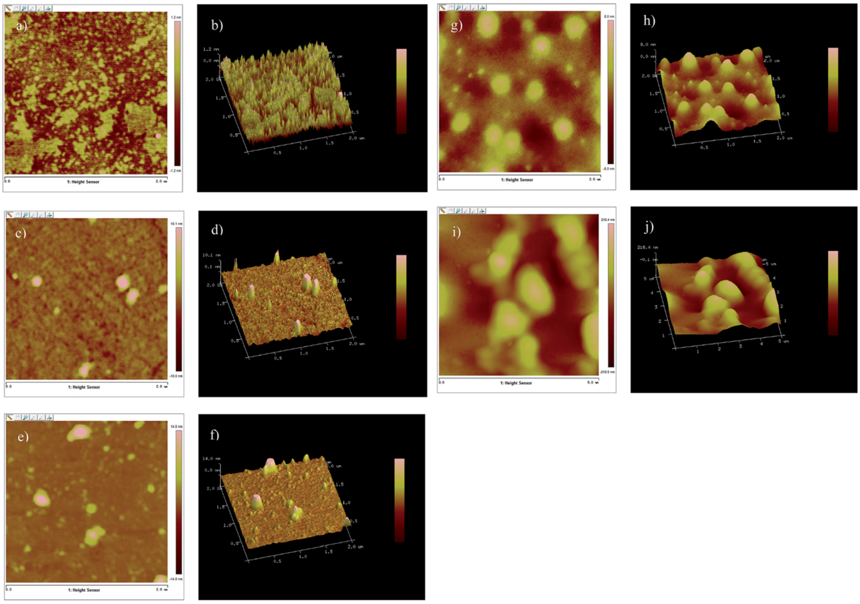

Fig. 2 AFM images of TMPU-321 thin films prepared by mixed solutions of different water fractions: (a), (c), (e), (g) and (i) are high contrast images at water fraction = 0%, 20%, 40%, 60%, and 80%, respectively; (b), (d), (f), (h) and (j) are the corresponding 3D high contrast images of (a), (c), (e), (g) and (i), respectively.

are about 40 nm, 130 nm, 200 nm, 230 nm and 1280 nm at 0%, 20%, 40%, 60%, and 80% water fraction (as shown in Table S1†), respectively, which are also identified by the SEM images in Fig. S5.† The AFM images give direct evidence that polyurethanes self-assemble into nanoparticles in DMF-water mixed solutions. TMPU-211 and TMPU-431 also present the same trend as given in their AFM images in Fig. S6 and S7.†

Due to the hydrophobic property of the soft segments in the resulting polyurethanes, these modified polyurethanes are inclined to aggregate as micelles, especially spherical micelles, in DMF-water mixed solution. Among the three polyurethanes, TMPU-431 has the biggest content of hydrophobic soft segments at a ratio of 3 : 1, which is most likely to form particles in the presence of water, leading to the highest relative fluorescence intensity change. However, nanoparticles formed in the polyurethane solutions would settle down when their diameters increase up to the order of a micron, thus causing the falling back of fluorescence intensity of the three polyurethane solutions at higher water fractions.

3.3 The effect of condensed structure on the fluorescence emission of the AEE polyurethane films

AEE films made from three modified polyurethanes were prepared in a PTFE mold and their FL spectra are shown in Fig. 3. Following preparation, the films underwent quenching treatments and an annealing process, which changed the condensed states of the soft segments. The spectra of the thermally-treated

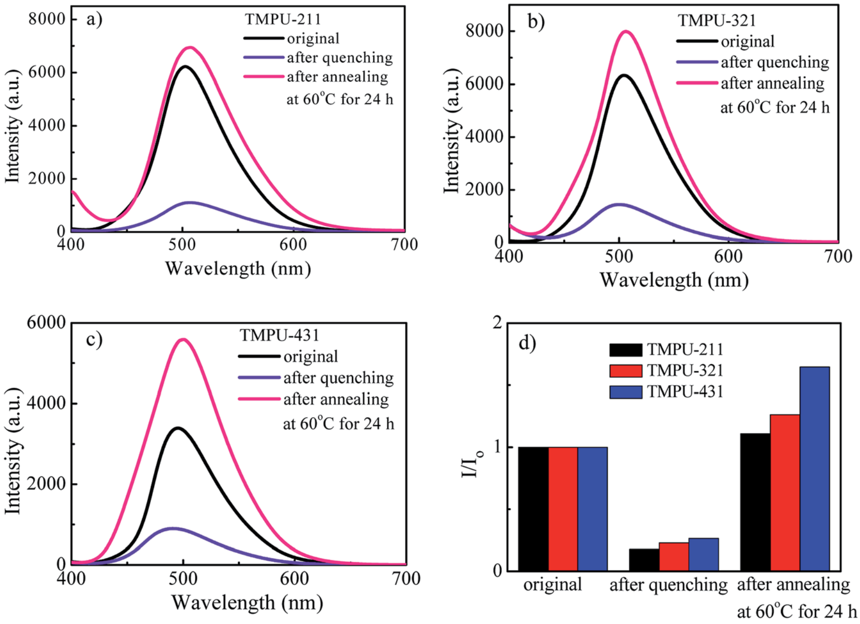

Fig. 3 Fluorescence emission spectra of: (a) TMPU-211, (b) TMPU-321, and (c) TMPU-431; (d) relative fluorescence intensity changes of the three polyurethane films before and after heat treatment.

films are also shown in Fig. 3. It can be seen from Fig. 3d that the fluorescence intensities of the TMPU-211, TMPU-321 and TMPU-431 films after quenching treatment decrease sharply. Then the fluorescence intensities of these films overtake and surpass those of the original films after annealing in the oven at 60 °C for 24 h. In addition, the fluorescence intensity change becomes more obvious after annealing treatment with the increase of the soft segment proportion in the polyurethanes.

To obtain deeper insight into these AEE polyurethane films, DSC tests were carried out to evaluate the thermal properties of the three polyurethanes. As shown in Fig. 4a–c, there are broad peaks in the range of 40–90 °C in the original state, which were assigned to the melting points of the soft segments of the three polyurethanes. These peaks disappear after quenching treatment, proving that the polyurethanes after quenching treatment possess an irregular soft segment structure and result in the decrease of fluorescence intensity. Then the melting peaks appear again and become more apparent after heat treatment, which means that heat treatment can rearrange the soft segments to form a more regular structure. More importantly, melting peak changes before and after annealing treatment become more apparent with the increase of soft segment proportion in the three polyurethanes, which correspond to the changes of fluorescence intensity in Fig. 3d. Polyurethanes with more soft segments have a larger proportion of regular structure after the annealing treatment, leading to the restriction of intramolecular rotation of the phenyl rotors in

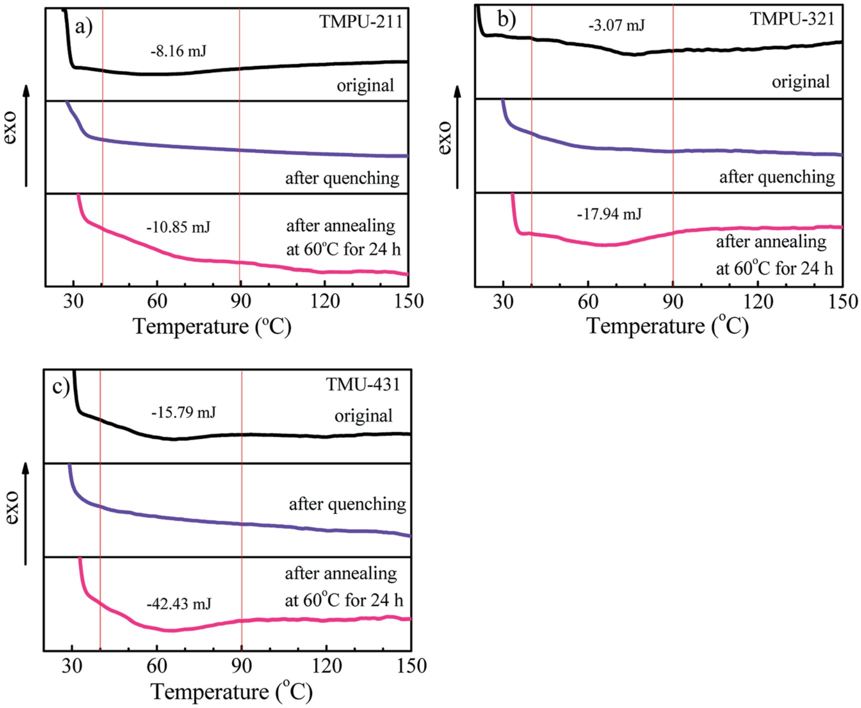

Fig. 4 DSC traces of (a) TMPU-211, (b) TMPU-321, and (c) TMPU-431 before and after the heat treatments.

the TABDAA moiety and consequently the large enhancement of the luminescence intensity.

Furthermore, AFM was used to investigate the molecular arrangement and microstructure of the AEE polyurethane films. All of these thin films were prepared by drop coating in a Teflon mold and evaporation in a constant temperature and humidity test chamber at 26 °C for 24 h. Fig. 5a–c are the phase image, high contrast image and 3D high contrast image of the original TMPU-321 films and Fig. 5d–f reflect the heat-treated TMPU-321 films, respectively. They indicate that TMPU-321 decorated on the glass surface can self-assemble into a nanoporous structure, and show a certain microphase separation. Fig. 5d–f show that the TMPU-321 films after annealing have formed more well-organized microphase separation morphologies. Since a polymer matrix with a more regular condensed structure has a tighter restriction effect on AIE moieties, this hinders intramolecular rotation and promotes the emission intensity of the AEE polymers. As a result, the condensed structure of the polymer matrix had a positive effect on the fluorescence intensity of the AEE polymers.

In summary, the different soft segment ratios of the polyurethanes lead to different aggregation states in the mixture solutions owning to the hydrophobicity of the soft segments, which affects the fluorescence intensities of the three modified polyurethane solutions. Meanwhile, heat treatment can rearrange the condensed structure of the soft segments, thus impacting the fluorescence intensities of the polyurethane films. Furthermore, the organized structure of the polymer matrix can improve the fluorescence emissions of AEE polymers and promote their application in fluorescent probes, stimuli-responsive materials, PLED devices and so on.

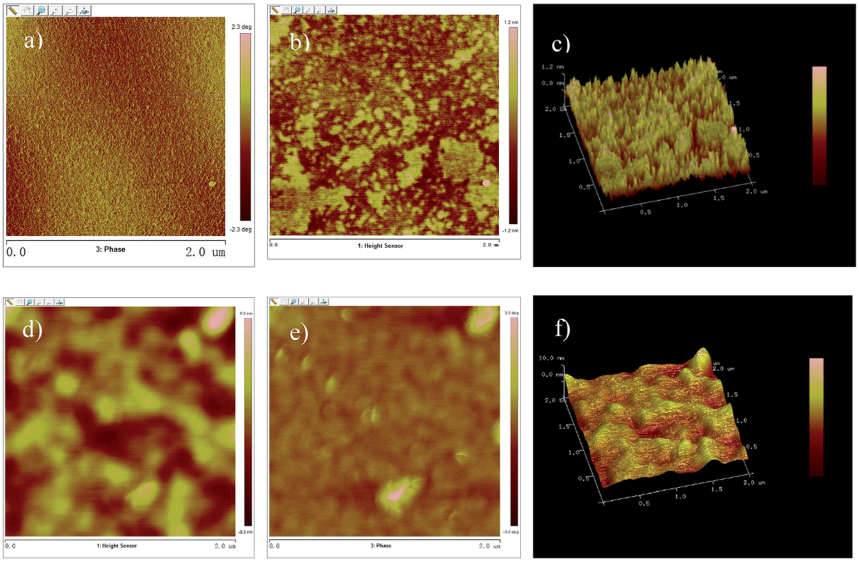

Fig. 5 (a–c): AFM images including phase image, high contrast image and 3D high contrast images of the original TMPU-321 thin films, respectively; (d–f): AFM images including phase image, high contrast image and 3D high contrast image of the TMPU-321 thin films after heat treatment, respectively.

4. Conclusions

In this paper, we synthesized three AEE polyurethanes abbreviated as TMPU-211, TMPU-321 and TMPU-431, based on the TABDAA moiety, with different soft/hard segment ratios. TMPU-431 with the highest soft segment proportion had the highest amplification of fluorescence intensity with the addition of water to the polyurethane DMF solution. Then the soft segment including TABDAA in the polyurethane films underwent quenching treatment and thermal annealing successively; the fluorescence intensity of the polyurethane films declined sharply and then ascended to a state even higher than the original. Heat treatment led to a more regular arrangement of the structure which produced a higher fluorescence intensity. To summarize, the structure of the polymer matrix, such as the soft/hard segment ratio and separation status, is an important factor in the fluorescence emission of the AIE/AEE polymers.

Acknowledgements

This work was supported by the National Natural Science Foundation of China (Grant No. 21174009, 21574003).

References

1 J. Luo, Z. Xie, J. W. Y. Lam, L. Cheng, B. Z. Tang, H. Chen, C. Qiu, H. S. Kwok, X. Zhan, Y. Liu and D. Zhu, *Chem. Commun.*, 2001, 1740–1741.
2 Y. Dong, J. W. Y. Lam, A. Qin, J. Liu, Z. Li, B. Z. Tang, J. Sun and H. S. Kwok, *Appl. Phys. Lett.*, 2007, **91**, 011111.
3 C.-T. Lai, R.-H. Chien, S.-W. Kuo and J.-L. Hong, *Macromolecules*, 2011, **44**, 6546–6556.
4 C. Y. K. Chan, J. W. Y. Lam, Z. Zhao, C. Deng, S. Chen, P. Lu, H. H. Y. Sung, H. S. Kwok, Y. Ma, I. D. Williams and B. Z. Tang, *ChemPlusChem*, 2012, **77**, 949–958.
5 C. Ma, Q. Ling, S. Xu, H. Zhu, G. Zhang, X. Zhou, Z. Chi, S. Liu, Y. Zhang and J. Xu, *Macromol. Biosci.*, 2014, **14**, 235–243.
6 H. Zhou, Q. Ye, W. T. Neo, J. Song, H. Yan, Y. Zong, B. Z. Tang, T. S. Hor and J. Xu, *Chem. Commun.*, 2014, **50**, 13785–13788.
7 P. Y. Gu, Y.-H. Zhang, D.-Y. Chen, C. J. Lu, F. Zhou, Q.-F. Xu and J. M. Lu, *RSC Adv.*, 2015, **5**, 8167–8174.
8 Y. Zhao, Y. Wu, G. Yan and K. Zhang, *RSC Adv.*, 2014, **4**, 51194–51200.
9 W. Dong, Y. Pan, M. Fritsch and U. Scherf, *J. Polym. Sci., Part A: Polym. Chem.*, 2015, **53**, 1753–1761.
10 Y. Guo, X. Feng, T. Han, S. Wang, Z. Lin, Y. Dong and B. Wang, *J. Am. Chem. Soc.*, 2014, **136**, 15485–15488.
11 Y. Liu, M. Gao, J. W. Y. Lam, R. Hu and B. Z. Tang, *Macromolecules*, 2014, **47**, 4908–4919.
12 H. Deng, E. Zhao, H. Li, J. W. Y. Lam and B. Z. Tang, *Macromolecules*, 2015, **48**, 3180–3189.
13 S. K. Saha, K. R. Ghosh, J. P. Gao and Z. Y. Wang, *Macromol. Rapid Commun.*, 2014, **35**, 1592–1597.
14 K. R. Ghosh, S. K. Saha and Z. Y. Wang, *Polym. Chem.*, 2014, **5**, 5638.

15 S. Zhang, Y. Sheng, G. Wei, Y. Quan, Y. Cheng and C. Zhu, *Polym. Chem.*, 2015, **6**, 2416–2422.
16 H. Deng, R. Hu, A. C. S. Leung, E. Zhao, J. W. Y. Lam and B. Z. Tang, *Polym. Chem.*, 2015, **6**, 4436–4446.
17 H. Deng, R. Hu, E. Zhao, C. Y. K. Chan, J. W. Y. Lam and B. Z. Tang, *Macromolecules*, 2014, **47**, 4920–4929.
18 C. T. Lai and J. L. Hong, *J. Phys. Chem. B*, 2010, **114**, 10302–10310.
19 H. J. Yen, C. J. Chen and G. S. Liou, *Chem. Commun.*, 2013, **49**, 630–632.
20 T. Han, Y. Zhang, X. Feng, Z. Lin, B. Tong, J. Shi, J. Zhi and Y. Dong, *Chem. Commun.*, 2013, **49**, 7049–7051.
21 Y. Zhang, T. Han, S. Gu, T. Zhou, C. Zhao, Y. Guo, X. Feng, B. Tong, J. Bing, J. Shi, J. Zhi and Y. Dong, *Chem.–Eur. J.*, 2014, **20**, 8856–8861.
22 J. Debabrata and B. K. Ghorai, *Tetrahedron Lett.*, 2012, **53**, 6838–6842.
23 J.-H. Li, Y. Liang and Y.-X. Xie, *J. Org. Chem.*, 2004, **69**, 3.